UC Santa Barbara
UC Santa Barbara Previously Published Works

Title
Quantification of trap densities at dielectric/III–V semiconductor interfaces

Permalink
https://escholarship.org/uc/item/0wd245s5

Journal
Applied Physics Letters, 97(6)

Author
Stemmer, Susanne

Publication Date
2010

DOI
10.1063/1.3479047

Peer reviewed

eScholarship.org Powered by the California Digital Library
University of California

APPLIED PHYSICS LETTERS **97**, 062905 (2010)

Quantification of trap densities at dielectric/III–V semiconductor interfaces

Roman Engel-Herbert,[a] Yoontae Hwang, and Susanne Stemmer[b]
Materials Department, University of California, Santa Barbara, California 93106-5050, USA

(Received 4 May 2010; accepted 20 July 2010; published online 10 August 2010)

High-frequency capacitance-voltage curves for capacitors with high-k gate dielectrics and III–V semiconductor channels are modeled. The model takes into account the low conduction band density of states, the nonparabolicity of the Γ valley, and the population of higher lying conduction band valleys. The model is used to determine interface trap densities (D_{it}) and band bending of $HfO_2/In_{0.53}Ga_{0.47}As$ interfaces with different D_{it} and with pinned and unpinned Fermi levels, respectively. Potential sources of errors in extracting D_{it} are discussed and criteria that establish unpinned interfaces are developed. © *2010 American Institute of Physics*. [doi:10.1063/1.3479047]

Compound (III–V) semiconductors, such as $In_{0.53}Ga_{0.47}As$, are currently under investigation to replace Si as the channel material in metal-oxide-semiconductor field-effect transistors (MOSFETs). A major obstacle in realizing III–V MOSFETs is the high density of traps (D_{it}) at the interface between the gate dielectric and the III–V semiconductor. Furthermore, to develop high-quality interfaces, methods to quantify D_{it} and the degree of Fermi level pinning are required. The conductance method, which has been widely used, provides reliable D_{it} estimates only around midgap, because the trap response is strongly temperature dependent.[1,2] Furthermore, accurate measures of the D_{it} can only be obtained for $C_{ox} > qD_{it}$, where C_{ox} is the capacitance density of the dielectric and q the elemental charge.[3] An alternative approach is the Terman method,[4,5] which is based on measuring the high-frequency capacitance-voltage (CV) characteristics of a metal-oxide-semiconductor capacitor (MOSCAP). The interface trap occupancy changes with gate bias, causing stretch-out of the CV curve. The stretch-out (or $d\psi_s/dV_g$, where ψ_s the semiconductor band bending and V_g the applied gate voltage) is obtained from comparison with an ideal CV curve (no D_{it}) and allows for quantification of the D_{it} as follows:[5]

$$D_{it}(\psi_s) = \frac{C_{ox}}{q}\left[\left(\frac{d\psi_s}{dV_g}\right)^{-1} - 1\right] - C_s(\psi_s), \quad (1)$$

where $C_s(\psi_s)$ is the ideal semiconductor capacitance. While a large frequency dispersion is often observed for high-k/III–V interfaces, modeling of the frequency dispersion shows that a measured 1 MHz high-frequency curve is sufficiently close to the ideal high-frequency curve to allow for the application of the Terman method.[6] For high-k/III–V interfaces, the ideal CV curve cannot be calculated "classically" as for dielectric-Si interfaces,[7] i.e., with the electron distribution given by the Boltzmann statistics.[5,8] The latter is valid only if the Fermi level remains inside the semiconductor band gap for all gate biases. For III–V MOSCAPs, the Fermi level moves deep into the conduction band,[7] because of the low conduction band density of states (DOS).[9] In addition, the nonparabolicity of the Γ valley and population of the higher lying valleys at X and L must be taken into account in modeling $C_s(\psi_s)$.

In this letter, the Terman method is developed for high-k/III–V interfaces and applied to $HfO_2/In_{0.53}Ga_{0.47}As$ interfaces. We discuss potential sources of errors in the application of the method and develop criteria to establish Fermi level unpinning at high-k/III–V interfaces.

To apply Eq. (1), $C_s(\psi_s)$ is calculated:

$$C_s(\psi_s) = -\frac{dQ_s(\psi_s)}{d\psi_s}. \quad (2)$$

The total charge Q_s per unit area in the semiconductor is obtained from the electrostatic potential, $\varphi(x)=(E_F-E_I)/q$, where E_F is the extrinsic Fermi level and E_I is the intrinsic energy level of the semiconductor. The Poisson equation relates the electrostatic potential to the charge density $\rho(x)$:

$$\frac{d^2\varphi(x)}{dx^2} = -\frac{\rho(x)}{\varepsilon_s} = -\frac{q\{p[\varphi(x)] - n[\varphi(x)] + N_D - N_A\}}{\varepsilon_s}, \quad (3)$$

where N_D and N_A are the donor and acceptor concentrations, respectively, ε_s is the semiconductor dielectric constant and $p[\varphi(x)]$ and $n[\varphi(x)]$ are the hole and electron densities, respectively, which depend on the electrostatic potential:

$$n[\varphi(x)] = \frac{4}{\sqrt{\pi}}\left(\frac{2\pi k_B T}{h^2}\right)^{3/2} \sum_{i=\Gamma,L,X} m_i^{*3/2} \times \int_0^\infty \frac{\sqrt{\eta_i}(1+\alpha_i\eta_i)(1+2\alpha_i\eta_i)}{\exp\left[\eta_i - \frac{q\varphi(x)}{k_B T} + \delta_i\right] + 1} d\eta_i, \quad (4)$$

where α_i is the nonparabolicity factor for valley i, $\eta_i = (E - E_i)/k_B T$ the normalized electron kinetic energy, and $\delta_i = (E_i - E_I)/k_B T$ the reduced energy band offset with respect to E_I. The effective DOS mass and the energies of valley i are m_i^* and E_i. Population of the different valleys is taken into account by the sum over Γ, L, and X. For the hole density the corresponding expression includes only a single valley and parabolic energy dispersion ($\alpha \to 0$), reflecting the higher DOS of the valence band and large split-off energy. For the values used in the calculation, see Ref. 10. Integration of Eq. (3) gives the electric field at the semiconductor surface $E[\varphi(x=0)]$ and applying Gauss' law yields the total charge Q_s per unit area in the semiconductor as follows:

[a]Electronic mail: rue2@psu.edu.
[b]Electronic mail: stemmer@mrl.ucsb.edu.

 © 2010 American Institute of Physics

Author complimentary copy. Redistribution subject to AIP license or copyright, see http://apl.aip.org/apl/copyright.jsp

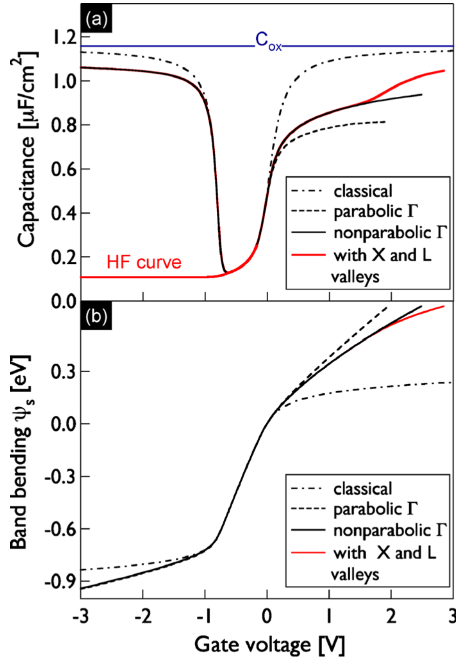

FIG. 1. (Color online) (a) Ideal, calculated, high and low frequency CV curves and (b) band bending as a function of gate voltage for different conduction band approximations. The dopant concentration is $N_D = 10^{17}$ cm^{-3} and the oxide capacitance $C_{ox} = 1.15$ μF/cm^2.

$$Q_s(\psi_s) = \varepsilon_s E[\varphi(x=0)]$$
$$= -\,\mathrm{Sign}(\psi_s)\sqrt{2\int_{\varphi_b}^{\varphi_b+\psi_s} - q\varepsilon_s\{N_D - N_A + p[\varphi(x)] - n[\varphi(x)]\}d\varphi(x)}, \tag{5}$$

where $\psi_s = \varphi_s - \varphi_b$ is the total band bending in the semiconductor, defined as the potential difference at the semiconductor surface φ_s with respect to the bulk potential φ_b. The total capacitance of the ideal MOSCAP is given by the following:

$$\frac{1}{C_{tot}} = \frac{1}{C_{ox}} + \frac{1}{C_s(\psi_s)}. \tag{6}$$

The gate voltage resulting in a band bending ψ_s is calculated

$$V_g = \psi_s + \Delta\phi_{ms} - \frac{Q_s(\psi_s)}{C_{ox}}, \tag{7}$$

where $\Delta\phi_{ms}$ is the work function difference between gate metal and semiconductor.[5]

Figures 1(a) and 1(b) show the total capacitance and band bending as a function of gate bias calculated from Eqs. (6) and (7) for a donor concentration $N_D = 10^{17}$ cm^{-3} and an equivalent oxide thickness (EOT) of 3 nm ($C_{ox} = 1.15$ μF/cm^2). The high frequency CV curve in inversion was calculated as described in Ref. 8 by taking the ac inversion layer polarization effect into account. In depletion, the high and low frequency capacitances are in good agreement. For comparison, also shown are CV and band bending calculated using the "classical" approximation,[5,8] for a parabolic Γ in Eq. (4) and with Γ nonparabolicity but neglecting the population of the X and L valleys, respectively. The different approximations strongly affect the CV in accumulation. The classical CV curve does not reveal the asymmetry due to the different valence and conduction band DOS. The parabolic Γ valley approximation underestimates the semiconductor capacitance and overestimates the asymmetry because it underestimates the increase in Q_s with band bending (at 1 V Q_s is underestimated by 25%). The parabolic approximation overestimates the band bending in accumulation [Fig. 1(b)]. In depletion and weak inversion Q_s is governed by the immobile donors and details of the band approximation do not affect band bending-gate voltage relationship. The population of the higher lying valleys results in an upturn of the CV curve for gate voltages exceeding 1.5 V, or a positive band bending larger than 0.4 eV.

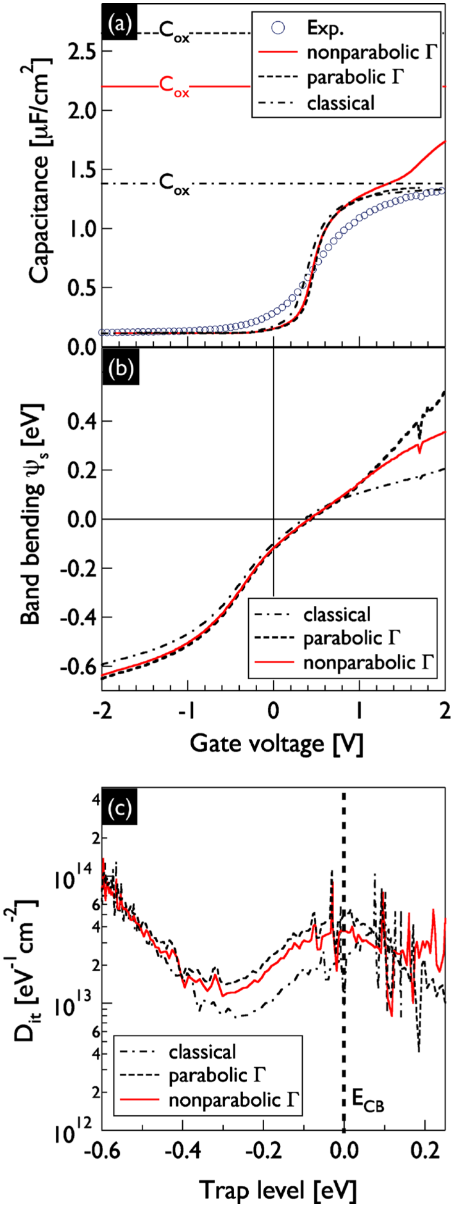

FIG. 2. (Color online) (a) Comparison of an experimental 1 MHz CV curve of a forming gas annealed MOSCAP with 9 nm HfO_2 (symbols) with modeled CV curves. The different models use nonparabolic and parabolic Γ valley approximations, respectively. The nonparabolic curve includes the occupation of higher lying conduction band valleys. Also shown is a "classical" CV curve (dashed-dotted line). The horizontal lines indicate the C_{ox} values obtained from comparison of experimental and modeled curves. (b) Experimental band bending obtained from comparisons of experimental and modeled CVs. (c) Extracted D_{it} for the different models.

The Terman method is applied to experimental 1 MHz CV curves of Pt/HfO_2/$In_{0.53}Ga_{0.47}As$ gate stacks with different D_{it}, as shown in Figs. 2 and 3. The HfO_2 films were grown by chemical beam deposition on n-doped (Si: 1×10^{17} cm^{-3}) $In_{0.53}Ga_{0.47}As$ as described elsewhere.[2,11] CV

Author complimentary copy. Redistribution subject to AIP license or copyright, see http://apl.aip.org/apl/copyright.jsp

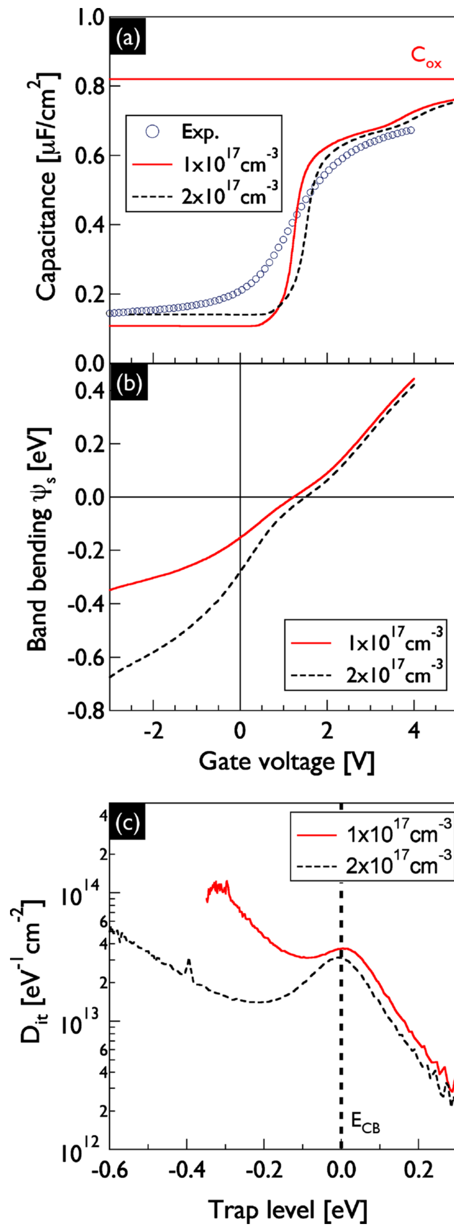

FIG. 3. (Color online) (a) Comparison of an experimental 1 MHz CV curve of a nitrogen gas annealed MOSCAP with 18 nm HfO_2 (symbols) with modeled CV curves using the nonparabolic Γ valley approximation. The modeled CVs are for a donor concentration of 1×10^{17} cm^{-3} (solid red line), which corresponds to the experimental concentration and a donor concentration of 2×10^{17} cm^{-3} (dashed black line), respectively. (b) Experimental band bending obtained from comparisons of experimental and modeled CVs. (c) Extracted D_{it}.

measurements were performed at room temperature as a function of postdeposition annealing atmosphere, which affects the degree of Fermi level pinning and D_{it}.[11] Figure 2 shows experimental and ideal CVs for the different approximations [Fig. 2(a)], extracted band bending [Fig. 2(b)], and D_{it} [Fig. 2(c)] for a 9 nm HfO_2 film annealed in forming gas. The band bending exceeds half the band gap of $In_{0.53}Ga_{0.47}As$ at the maximum applied negative voltage, indicating an unpinned Fermi level. It is best practice (see below) to use the accumulation capacitance to match the ideal CV curve to the experimental curve. C_{ox} is estimated to be 2.20 μF/cm^2 for this stack, resulting in a minimum D_{it} of 1.14×10^{13} eV^{-1} cm^{-2}. The estimated C_{ox} agrees well that estimated from the dielectric constant obtained using a thickness series.[2] Using the parabolic Γ or classical approximations result in incorrect estimates for C_{ox}. Errors in C_{ox}, which scale with EOT, lead to errors in the extracted D_{it} [see Eq. (1)]. The classical approximation underestimates C_{ox} [dashed-dotted line in Fig. 2(a)] causing the extracted D_{it} to be much lower than its actual value. The apparent upturn in D_{it} near the valence band [Fig. 2(c)] is an artifact of the Terman method; as the slope of the CV curve decreases in depletion, errors in extracting the D_{it} become too large to yield reliable results.

Figure 3 shows the analysis for a 18 nm HfO_2 film annealed in nitrogen. For this stack, the capacitance at negative gate bias does not reach the minimum capacitance [solid red line in Fig. 3(a)], indicating that the semiconductor is not fully depleted because the Fermi level is pinned around midgap. Furthermore, the band bending near midgap is limited [Fig. 3(b)]. In contrast to the forming gas annealed stack [Fig. 2(c)], this stack shows a D_{it} peak near midgap. Forming gas anneals reduce midgap D_{it} by an order of magnitude, as comparison of the solid red lines in Figs. 2(c) and 3(c) shows. For stacks with a pinned Fermi level, fitting the ideal CV curve to the minimum capacitance [as is done for the dashed curve in Fig. 3(a)] is not good practice. It causes an overestimation of the dopant concentration, stretching the ideal CV curve, resulting in a severe overestimation of the band bending [dashed curve in Fig. 3(b)], leading to incorrect claims of Fermi level unpinning, and underestimation of D_{it} [dashed curve in Fig. 3(c)].

The results show that the Terman method gives reliable estimates of D_{it} and band bending provided that the details of the semiconductor band structure are correctly modeled and the semiconductor dopant concentration is known. For n-type channels, the Terman method can be used to establish Fermi level unpinning around midgap. In particular, the minimum high frequency capacitance must match the calculated value for the given dopant concentration and the band bending must exceed half of the semiconductor band gap.

The authors thank funding from the Semiconductor Research Corporation through the Nonclassical CMOS Research Center (Task ID 1437.005). R.E.H. thanks O. Bierwagen for valuable discussions.

[1] K. Martens, C. O. Chui, G. Brammertz, B. De Jaeger, D. Kuzum, M. Meuris, M. Heyns, T. Krishnamohan, K. Saraswat, H. E. Maes, and G. Groeseneken, IEEE Trans. Electron Devices **55**, 547 (2008).

[2] Y. Hwang, R. Engel-Herbert, N. G. Rudawski, and S. Stemmer, Appl. Phys. Lett. **96**, 102910 (2010).

[3] H. C. Lin, G. Brammertz, K. Martens, G. de Valicourt, L. Negre, W.-E. Wang, W. Tsai, M. Meuris, and M. Heyns, Appl. Phys. Lett. **94**, 153508 (2009).

[4] L. M. Terman, Solid-State Electron. **5**, 285 (1962).

[5] E. H. Nicollian and J. R. Brews, *MOS (Metal Oxide Semiconductor) Physics and Technology* (Wiley, New York, 1982).

[6] A. Ali, H. Madan, S. Koveshnikov, S. Oktyabrsky, R. Kambhampati, T. Heeg, D. Schlom, and S. Datta, IEEE Trans. Electron Devices **57**, 742 (2010).

[7] G. Brammertz, H. C. Lin, M. Caymax, M. Meuris, M. Heyns, and M. Passlack, Appl. Phys. Lett. **95**, 202109 (2009).

[8] J. R. Brews, J. Appl. Phys. **45**, 1276 (1974).

[9] T. Yang, Y. Liu, P. D. Ye, Y. Xuan, H. Pal, and M. S. Lundstrom, Appl. Phys. Lett. **92**, 252105 (2008).

[10] See supplementary material at http://dx.doi.org/10.1063/1.3479047 .

[11] Y. Hwang, R. Engel-Herbert, N. G. Rudawski, and S. Stemmer, "Effect of postdeposition anneals on the Fermi level response of $HfO_2/In_{0.53}Ga_{0.47}As$ gate stacks," J. Appl. Phys.(to be published).

Author complimentary copy. Redistribution subject to AIP license or copyright, see http://apl.aip.org/apl/copyright.jsp